Broadly neutralizing plasma antibodies effective against diverse autologous circulating viruses in infants with multivariant HIV-1 infection.

Nitesh Mishra[1†], Shaifali Sharma[1†], Ayushman Dobhal[1†], Sanjeev Kumar[1‡], Himanshi Chawla[1§], Ravinder Singh[2], Muzamil Ashraf Makhdoomi[1||], Bimal Kumar Das[2], Rakesh Lodha[3], Sushil Kumar Kabra[3], Kalpana Luthra[1]*.

[1]Department of Biochemistry, All India Institute of Medical Sciences, New Delhi, India – 110029.
[2]Department of Microbiology, All India Institute of Medical Sciences, New Delhi, India – 110029.
[3]Department of Pediatrics, All India Institute of Medical Sciences, New Delhi, India – 110029.

[†]These authors contributed equally to this work.

[‡]Current Address – International Centre for Genetic Engineering and Biotechnology, New Delhi, India.

[§]Current Address – Biological Sciences and the Institute for Life Sciences, University of Southampton, Southampton, SO17 IBJ, United Kingdom.

[||]Current Address – Department of Biochemistry, Government College for Women, Cluster University, Srinagar, Srinagar, India.

*Correspondence – Kalpana Luthra (kalpanaluthra@gmail.com)

Abstract

Due to the extensive antigenic diversity of human immunodeficiency virus-1 (HIV-1), broadly neutralizing antibodies (bnAbs) develop in a subset of infected individuals over 2-3 years of infection. Interestingly, infected infants have been shown to develop plasma bnAbs frequently and as early as one-year post-infection, with features atypical than adult bnAbs, suggesting that the factors governing bnAb induction in infants are distinct from that in adults. Understanding the viral characteristics in infected infants with early bnAb responses will provide key information on the antigenic triggers driving B cell maturation pathways towards the induction of bnAbs. Herein, we evaluated the presence of plasma bnAbs in a cohort of 51 HIV-1 clade C perinatally infected infants of Indian origin and identified viral factors associated with early bnAb responses. Plasma bnAbs targeting V2-apex on the env were predominant in infant elite and broad neutralizers. Circulating viral variants in infant elite neutralizers were susceptible to known bnAbs against V2-apex while varied resistance profile to other bnAb classes was observed. In infant elite neutralizers, multivariant infection was associated with plasma bnAbs targeting diverse autologous viruses. Our data provides information supportive of polyvalent vaccination approaches capable of inducing V2-apex bnAbs against HIV-1.

Introduction

An effective human immunodeficiency virus – 1 (HIV-1) vaccine that can curtail the AIDS pandemic is the need of the hour. The HIV-1 envelope glycoprotein (env), is a trimer of non-covalently linked

36 heterodimers $(gp120/gp41)_3$, and is the primary target of broadly neutralizing antibodies (bnAbs).
37 The bnAbs are capable of neutralizing diverse circulating variants of HIV-1 and are generated in rare
38 subsets of infected individuals. Passive administration of such bnAbs in animal models and in
39 recently conducted human clinical trials with bnAbs alone, or in combination with antiretroviral
40 therapy, have shown protection from HIV-1 infection [1,2]. HIV-1 bnAbs are categorized based on their
41 recognition of five distinct and largely conserved epitopes on the envelope spike that are promising
42 vaccine targets: the N160 glycan located within the V2 loop at the trimer apex (V2-apex), high
43 mannose patch centered around N332 in the V3 region, the CD4 binding site (CD4bs), the membrane
44 proximal external region (MPER), and the N-glycans located at the gp120–gp41 interface [1,2]. A
45 prolonged exposure to the viral env during natural infection has been implicated as a prerequisite
46 for the development of broadly neutralizing antibodies (bnAbs) capable of neutralizing diverse viral
47 strains, as is observed in select HIV-1-infected adults, who develop such bnAbs after a minimum of
48 two to three years of infection [3–6].

49 In HIV-1 infected children, plasma bnAbs arise earlier in infection, and show higher potency and
50 breadth compared to adults [7–11]. We observed the presence of cross-neutralizing antibodies in HIV-1
51 clade C chronically infected children [11] and recently generated a bnAb AIIMS-P01 from an elite
52 pediatric neutralizer AIIMS_330 [12]. Further in this cohort of chronically infected children, AIIMS_329
53 and AIIMS_330, a pair of identical twins, showed elite plasma neutralizing activity [13]. A longitudinal
54 analysis of the plasma antibody response and circulating viral strains showed the presence of diverse
55 circulating in both twins, with varied susceptibility to neutralization by plasma antibodies and bnAbs,
56 irrespective of their similar genetic makeup and source of infection. Studies undertaken in infants
57 have, however, documented that HIV-1 infected infants develop potent plasma bnAbs as early as
58 one-year post-infection [9,10] suggesting that an effective vaccine in infants may perhaps be able to
59 trigger the immune system and elicit an early bnAb response thus providing an impetus to evaluate
60 the antibody response in a cohort of perinatally infected infants. Moreover, the bnAbs isolated from
61 infected children show features atypical of adult bnAbs suggesting that the factors governing bnAb
62 induction in infants are distinct from those in adults [12,14].

63 Infants infected via mother-to-child transmission (MTCT), with the well-defined genetic bottleneck
64 leading to infection with a minor variant [15], provide a unique setting to understand the viral factors
65 associated with induction of bnAbs. Herein, we evaluated the characteristic features of circulating
66 viral strains in infants that show an early bnAb response to understand the antigenic triggers that
67 drive B cell maturation pathways towards induction of bnAbs.

68 **Results**

69 **Identification of HIV-1 infected infants with elite plasma neutralization activity**

70 In order to identify infants with potent plasma nAbs in our cohort of 51 infants, HIV-1 specific plasma
71 bnAb breadth was assessed. We first evaluated nonspecific inhibitory effect by assessing the
72 inhibition of MuLV infection in a TZM-bl based pseudovirus neutralization assay. Of the 51 plasma
73 samples, 4 showed nonspecific inhibitory effect and were excluded from further analysis. To identify
74 infants with early bnAb responses, we next performed plasma neutralization activity of the
75 remaining 47 infants against a panel of 12 genetically divergent pseudoviruses [16,17], representing
76 global viral diversity, in order to capture plasma bnAbs targeting diversity encountered in the
77 context of global HIV-1 pandemic. Cross-clade neutralization activity (CrNA), the ability to neutralize
78 non-clade C pseudoviruses (different clade than the infecting clade) at ID_{50} titers >50, was observed
79 in 19 of the 47 infants at a median time of 12-months post-infection (p.i.) (range = 6 – 24 months)
80 (**Fig. 1A**). Further, plasma neutralization activity against an 8-virus panel of Indian origin was
81 assessed [13,17]. While the geometric mean titres were comparable for infants with both the global
82 panel and Indian clade C panel, infants had higher breadth against Indian clade C panel (**Fig. S1A –**
83 **C**).

84 Though the plasma neutralization activity against the 12-virus global panel in infants was relatively
85 broad with 21% (10/47) of infants neutralizing ≥50% of the pseudoviruses, their potency in
86 comparison to plasma neutralization activity from previously characterized cohorts of chronically
87 infected children and adults from our lab showed relatively lower magnitude (**Fig. 1B and C**), which
88 prompted us to define pediatric elite neutralizers and broad neutralizers in the context of a modified
89 breadth-potency matrix. For infant plasma samples, percent neutralization for each plasma-virus
90 combination was recorded as a breadth-potency matrix at a fixed dilution of 1/50: >80%
91 neutralization received a score of 3, >50% a score of 2, >20% a score of 1, and <20 received a score
92 of 0. Maximum cumulative score for a given plasma was 36, and neutralization score was given as
93 the ratio of cumulative score for respective plasma to the maximum cumulative score, providing
94 neutralization score on a continuous matrix of 0 to 1, with values closer to 1 implying strong plasma
95 neutralization activity. The normalized neutralization scores, predictive of geometric mean titres and
96 cross-clade neutralization, were calculated (**Fig. 1D**). A cut-off of 0.7 defined the 90th-percentile
97 boundary and was used to define elite neutralizers (neutralizing ≥90% pseudoviruses), whereas a
98 cut-off of 0.3 (75th-percentile) was used to define broad neutralizers (neutralizing ≥50%
99 pseudoviruses) **(Fig. S2A – B**). The neutralization scores for known elite and broad neutralizers from
100 previously reported pediatric [11] and adult [18] cohorts were also calculated based on the same
101 modified breadth-potency matrix, and the normalized neutralization score defined herein could
102 categorize pediatric and adult elite and broad neutralizers (**Fig. S2B**). Based on this scoring system,

103 four infants were classified as elite neutralizers (AIIMS704, AIIMS706, AIIMS709, and AIIMS743) and
104 six infants as broad neutralizers (AIIMS731, AIIMS719, AIIMS736, AIIMS744, AIIMS732 and
105 AIIMS738) (**Table S1)**.

106 **V2-apex targeting bnAbs predominated in infants with elite and broad plasma neutralization**
107 **activity**

108 Next, to delineate the epitope specificities of the plasma bnAbs from these infant elite and broad
109 neutralizers, we used the HIV-25710_2_43 mutant pseudoviruses containing key mutations within
110 the epitope for V2-apex, V3-glycan, CD4bs, gp120-gp41 interface and MPER. The plasma bnAbs of
111 majority of the infants (8/10) were directed against the V2-glycan, with two elite neutralizers
112 (AIIMS704 and AIIMS706) showing multi-epitope dependency, a feature reported to be typically
113 associated with chronic antigenic exposure [8,13] (**Fig. 2A**). For AIIMS709 and AIIMS736, no
114 dependence on any of the five epitopes was observed. To further validate that the high frequency of
115 V2-apex targeting plasma nAbs were not specific to HIV-25710_2_43 pseudoviruses, infant plasmas
116 that showed V2-apex dependence were further mapped with 16055, CAP45 and BG505 N160A
117 mutant pseudoviruses (**Fig. 2B**). For AIIMS706, additionally, N332A mutants of BG505, CAP256 and
118 ConC were used as the plasma also had nAbs targeting V3-glycan (**Fig. 2C**). Though the extent of
119 dependence varied from one pseudovirus to another, the expanded mapping showed similar trend
120 as initial mapping done with HIV-25710_2_42, confirming high frequency of V2-apex plasma bnAbs
121 in this cohort of infants. Interestingly, in AIIMS704, in addition to V2-apex targeting plasma nAbs,
122 MPER dependence was also observed. MPER-directed bnAbs are rare in individuals with acute
123 infection, highlighting the uniqueness of our observation of MPER plasma bnAbs in a 12-month old
124 infant. To address whether the pan-neutralization of the global panel by AIIMS704 plasma nAbs
125 were MPER mediated or an additive effect of having two distinct plasma nAb specificity, we depleted
126 the MPER antibodies from AIIMS704, and checked the neutralization of global panel with MPER-
127 depleted AIIMS704 plasma. Depletion of MPER antibodies from plasma was confirmed by binding
128 ELISA against MPER-C peptide (**Fig. S3A – B**). MPER-depleted AIIMS704 plasma antibodies
129 neutralized 50% of the global panel (6/12), and showed a 2.14-fold reduction in GMT titres. All
130 circulating recombinant viruses from the global panel (246F3, BJOX2000, CH119, CNE8 and CNE55)
131 became resistant after depletion of MPER-specific plasma nAbs (**Fig. 2D, Fig. S3C**).

132 **Infants with elite neutralizing plasma bnAbs had multivariant HIV-1 infection**

133 We next focused our analysis on three parameters (viral load, CD4 count and duration of infection)
134 to identify factors driving bnAb induction. No significant association was observed between CD4
135 counts or duration of infection with neutralization breadth (**Fig. S4A – B**), suggesting that these

136 parameters did not influence bnAb induction in this cohort of infants. High viral load showed
137 negative correlation with neutralization breadth (r = -0.497, p = 0.002) (**Fig. S4C**). Another factor
138 influencing bnAb induction is the diversity in the viral envelope glycoprotein (env). Diversity in the
139 viral env generated as a result of immune selection pressure (neutralization escape) or
140 superinfection can independently drive bnAb induction [5,6,13]. To define viral diversity in the context
141 of bnAb induction, we performed SGA analysis of env sequences [19] (V2C5 region of HIV-1 gp120,
142 HXB2 position 6690 – 7757) from circulating viral variants in elite and broad neutralizers to assess
143 the impact of viral diversity on bnAb induction. From elite and broad neutralizers, a total of 377 env
144 gene sequences were obtained with more than 35 env sequences from each infant, giving a 90%
145 confidence interval of sequencing circulating variants present at 5% population frequency (**Table 1**
146 **and Table S2**). Sequences containing large deletions or G-to-A hypermutations were excluded. All
147 sequences were predicted to be clade C throughout the env gene reading frame, and had the
148 highest phylogenetic relatedness to the reference sequence C.IN.95IN21068.AF067155 (GenBank
149 accession number AF067155) complied in HIV database. Co-receptor usage was inferred based on V3
150 loop sequences, and all 377 sequences were predicted to use CCR5.

151 Sequences were aligned, visually inspected using the highlighter tool and maximum likelihood
152 phylogeny tree were generated to identify the pattern of viral transmission. Pairwise raw distance
153 distribution (nucleotide substitution per site) and env gene diversity (mean genetic distance) were
154 assessed to calculate the intra-host diversity. All four elite neutralizers (AIIMS704, AIIMS706,
155 AIIMS709 and AIIMS743) showed evidence of multivariant HIV-1 infection (distinct clusters on
156 highlighter plots and distinct branches on phylogeny tree with high degree of bootstrap support [20–
157 25]), with one infant, AIIMS709, showing two highly divergent variants, plausibly due to
158 superinfection, that needs to be further explored (**Fig. 3A – B, Fig. 4A – D**). SGA env sequences from
159 broad neutralizers (AIIMS731, AIIMS719, AIIMS736, AIIMS744, AIIMS732 and AIIMS738) were
160 monophyletic (**Fig. 3A**). Within-patient diversity in elite neutralizers ranged from 0.6 to 15.1 (**Table**
161 **1**). Such extent of within-patient diversity are typical of multivariant infections [19,21,22,24]. AIIMS709
162 had the maximum within-patient diversity, further confirming infection with highly divergent viruses.
163 For broad neutralizers, within-patient diversity ranged from 0.3 to 0.7, a feature typical of infection
164 with a single virus or multiple closely related viruses (**Table 1**). Significantly higher evolutionary
165 divergence (nucleotide substitutions per site) was observed in elite neutralizers compared to broad
166 neutralizers (p = 0.0095) (**Fig. S5A – B**). Moreover, the multivariant infection in this infant cohort was
167 significantly associated (odds ratio >35, p = 0.043) with development of plasma breadth, though a
168 small sample size might have skewed the association.

169 **Contemporaneous plasma bnAbs are effective against autologous circulating viruses in infant elite**
170 **neutralizers**

171 To gain insight and evaluate the impact of multivariant infection and decipher viral characteristics
172 associated with the development of plasma nAbs in infant elite neutralizers, we next generated
173 functional pseudoviruses from all four infant elite neutralizers. The generated pseudoviruses were
174 tested for neutralization by autologous nAbs. Distinct viral populations in each of the infected infant
175 showed varied susceptibility to autologous plasma nAbs, with several variants sensitive and others
176 moderately sensitive to autologous plasma bnAbs (**Fig. 5A**), an observation we previously reported
177 to be a plausible driver of elite plasma neutralization activity [13]. Moreover, none of the circulating
178 viral strains in four infants were resistant to autologous plasma nAbs. In addition, susceptibility of
179 the pseudoviruses from these infant elite neutralizers to known bnAbs and non-nAbs was also
180 assessed. Majority of the pseudoviruses showed similar neutralization susceptibility profile to V2-
181 apex targeting bnAbs while the susceptibility to other bnAb classes varied between pseudoviruses.
182 Notable sequence similarity was observed in the strand B and C of the V2-loop of the pseudoviruses
183 (**Fig. S6**). No reactivity was observed with non-nAbs for majority of the pseudoviruses, suggesting a
184 well-ordered trimeric configuration (**Fig. 5A**). To study the antigenic and conformational
185 characteristics of intact, native env trimers, we transiently transfected HEK293T cells with respective
186 env clones from each infant elite neutralizer that showed maximum susceptibility to autologous
187 plasma nAbs and the panel of known bnAbs. No effect of sCD4 on the binding of 2G12, which binds
188 an exposed glycan epitope on gp120, was observed suggesting CD4 binding did not induce gp120
189 dissociation (**Fig. 5B-E**). CD4-induced non-neutralizing antibodies, 17b and A32, that bind the open
190 trimer showed no binding and in presence of sCD4, only weak binding could be observed.
191 Predominant binding of trimer-specific bnAbs PGDM1400, and CAP256.25 was observed, though
192 binding of 10-1074 and PGT151 did vary between envs. The viral variants from these infant elite
193 neutralizers were susceptible to bnAbs, showed diverse susceptibility profile to autologous plasma
194 nAbs, and plausibly adopted closed trimeric conformations.

195 **Discussion**

196 Broadly neutralizing antibody (bnAbs) responses in HIV-1 infected adults have been well established,
197 whereas limited number of studies exist assessing these responses in HIV-1 infected children. Apart
198 from select studies, information on the neutralization activity of plasma antibodies in infants is
199 lacking. Herein, we observed cross-clade neutralizing activity in 42% of the infected infants, and even
200 though we used a less stringent cut-off of 1/50, the virus panel utilized in this study had a relatively
201 higher percentage of difficult to neutralize pseudoviruses (normalized tier scores of 2.5 to 3) [16,26]. In

202 the study conducted by Goo et. al. [9], 71% of the infected infants showed cross-clade neutralization.
203 Prevalence of crNA in HIV-1 infected individuals from different cohorts has been shown to be 10 to
204 30%. The GMT values observed in this study were on the lower side, plausibly due to limited
205 exposure to the antigen with a median infection duration of 12-months. Development of potent
206 plasma antibodies usually requires two to four years post-seroconversion, and is aided by chronic
207 antigen exposure [3,4,11,18,27].

208 Currently reported bnAbs primarily target five epitopes on env: glycan dependent sites within the V2
209 and V3 (V2-apex and V3-glycan) regions, CD4 binding site (CD4bs), gp120/gp41 interface, and
210 membrane proximal external region (MPER) [1,2]. The plasma antibodies of majority of the infants in
211 this study were found to be directed against the V2-apex. Despite the high variability in terms of the
212 sequence, glycosylation and length of the V2-apex of HIV-1 envelope, bnAbs directed against V2-
213 apex are elicited relatively early and are one of the most potent classes of bnAbs [1–4]. The findings
214 herein of a high frequency of V2-apex bnAbs in infants with cross-clade neutralization activity is in
215 consensus with previous observations in infected children [8]. Given the relatively higher frequency,
216 earlier induction, moderate level of somatic hypermutation, and consistent cross-clade neutralizing
217 activity of V2-apex bnAbs in conjunction with cross-species conservation of the epitope given its
218 critical function for trimer disassembly during viral entry [3,4,27–30], this bnAb epitope has been focus of
219 recent immunogen design approaches. Our results further support the notion for exploring V2-apex
220 targeting bnAbs, either as prophylactics or immunogen targeted induction, in the field of HIV-1
221 vaccinology. In two infant elite neutralizers, multi-epitope dependency was observed. Antibodies
222 targeting multiple epitopes in children have been reported, though chronic exposure has been
223 suggested as one of the mechanisms for the development of multiple antibody lineage.
224 Nevertheless, the exact factors that predispose children for the development of multiple bnAb
225 lineages are unknown and need to be addressed. Antibodies against MPER are rarely elicited in
226 children, plausibly due to the structural constraints in accessing the MPER as well as autoreactivity of
227 MPER bnAbs. Our findings of MPER nAbs in a 12-month old infant (AIIMS704) suggests similar bnAbs
228 can be induced early with targeted vaccination strategies that can plausibly overcome the linked
229 immune tolerance mechanisms blocking such nAbs.

230 Diversity in the viral env, either generated by immune selection pressure (neutralization escape) or
231 superinfection, has been shown to be an independent driver of bnAb induction [5,6,13]. In our cohort, a
232 significant association between multivariant infection and elite plasma neutralization activity was
233 seen, and though at the time of recruitment, all infants were in Fiebig stage VI, the extent of
234 diversity observed could not be explained with established models of mutations gained due to
235 escape mutations as a result of selection due to plasma nAbs [19,21,25]. Multivariant HIV-1 infection is

236 more commonly seen in adults than in children who have acquired the infection by vertical
237 transmission [19–21,31]. In both children and adults, the stringent genetic bottleneck for transmission
238 often leads to infection by a single viral variant [32–34]. HIV-1 multivariant infection is defined as one
239 person infected with two or more different HIV-1 strains. According to the timing of infection with
240 the second strain, multivariant infections can be divided into co-infection [33] (acquisition of a second
241 strain either simultaneously or before seroconversion) and superinfection [34,35] (acquisition of a
242 second strain after seroconversion), but given the cross-sectional nature of this study, we could only
243 categorically decipher the timeline of the multivariant infections, and hence used the broad term of
244 multivariant infection.

245 A better understanding of the mechanisms that determine the wide range of neutralization
246 sensitivity and antigenic landscape of circulating primary HIV-1 isolates would provide important
247 information about the natural structural and conformational diversity of HIV-1 env and how this
248 affects the neutralization phenotype. Circulating viruses in infected individuals who develop potent
249 plasma bnAbs characteristically develop resistance to autologous plasma nAbs as a result of the
250 mutations acquired due to immune selection pressure. Herein, the circulating viruses sensitive to
251 autologous plasma nAbs in all four elite neutralizers were observed. Interestingly, despite the
252 presence of V2-apex targeting plasma nAbs, circulating viral variants of AIIMS704, AIIMS706 and
253 AIIMS743 retained epitope-defining sequences and N-glycosylation sites at V2-apex. In addition,
254 epitope defining key residues for all bnAb classes (V2-apex, V3-glycan, CD4bs, gp120-gp41 interface
255 and MPER) were retained on circulating viruses from AIIMS704 and AIIMS706. A fundamental
256 challenge in HIV-1 vaccine strategy has been the development of native-like trimers capable of
257 expressing bnAb epitopes while occluding immune-dominant non-neutralizing antibody epitopes.
258 Preferential binding of bnAbs and not nnAbs has been correlated with efficient cleavage of env
259 gp160 polypeptide into its constituent subunits (gp120 and gp41). For immunogen design, efficient
260 cleavage of candidate envs is a desirable property. For majority of the envs from elite neutralizers,
261 CD4i targeting antibodies (17b, 48d and A32) showed negligible binding following sCD4 triggering
262 while trimer-specific bnAbs showed prominent binding, suggesting a stable and homogenous
263 conformational and antigenic state. In addition, recent line of evidence suggest that select HIV-1
264 viral variant have the capability to initiate bnAb responses [36]. Given that these infants generated
265 remarkable antibody response within a year of infection, envs from these infants can be explored as
266 potential immunogen candidates.

267 In this cross-sectional study on a small cohort of HIV-1 clade C infected infants, we have
268 demonstrated an association of multivariant infection with the development of plasma bnAb
269 response. Though exposure to two distinct viral variants in adults has been shown to be not

270 sufficient to broaden neutralizing antibody responses [37,38], our findings of an early bnAb response in
271 context of multivariant infection can be a distinct feature of infant immune response to HIV-1
272 infection. This needs to be validated in established cohorts of HIV-1 infected infants. Our data
273 provides key evidence for exploring polyvalent vaccination approaches for pediatric HIV-1 infection.
274 Polyvalent vaccines have been less explored due to immunodominance of HIV-1 which in turn can
275 diminish the efficacy of vaccines [39,40]. We observed the plasma nAbs in infants with multivariant
276 infection to target both variants, suggesting env specific antibodies generated in context of two
277 distinct viral variants can target epitopes on both envelopes. In addition, viral variants from these
278 infants can be explored as candidate priming immunogens to elicit V2-apex targeting bnAbs.
279 Furthermore, longitudinal analysis in established infant cohorts should be undertaken to understand
280 how the immune system in infants responds to multiple HIV-1 strains which will provide key insights
281 for guiding the early development of such bnAbs. To conclude, our results further add to a growing
282 body of literature suggesting infants may have different immunological tolerance mechanisms and
283 may be permissive for the development of bnAbs.

284 **Materials and Methods**

285 **Study design and participants**

286 The current study was designed to decipher the viral characteristics that influence the early
287 induction of plasma bnAbs in HIV-1 infected infants. Antiretroviral naïve and asymptomatic HIV-1
288 infected infants below the age of 2-years visiting the Pediatric Chest Clinic, Department of Pediatrics,
289 AIIMS during the duration of this study were recruited randomly. A total of 51 antiretroviral naïve
290 and asymptomatic HIV-1 infected infants were recruited for this study. After written informed
291 consent from guardians, blood was drawn in 3-ml EDTA vials, plasma was aliquoted for plasma
292 neutralization assays, viral RNA isolation, and viral loads. The study was approved by institute ethics
293 committee of All India Institute of Medical Sciences. The median age for infected infants was 12-
294 months (IQR, 8 – 19), the median CD4 count was 1731 cells/mm^{3-} (IQR, 1498 – 2562) and the median
295 viral load on log scale was 5.804 RNA copies/ml (IQR, 5.331 – 6.301).

296 **Plasmids, viruses, monoclonal antibodies, and cells**

297 Plasmids encoding HIV-1 env genes representing different clades, monoclonal antibodies and TZM-bl
298 cells were procured from NIH AIDS Reagent Program. 10-1074 and BG18 expression plasmids were
299 kindly provided by Dr. Michel Nussenzweig, Rockefeller University, USA. CAP256.09, CAP256.25 and
300 b6 were procured from IAVI Neutralizing Antibody Centre, USA. HEK293T cells were purchased from
301 the American Type Culture Collection (ATCC).

302 **Neutralization assay**

303 Neutralization assays were carried out using TZM-bl cells, a genetically engineered HeLa cell line that
304 constitutively expresses CD4, CCR5 and CXCR4, and contains luciferase and β-galactosidase gene
305 under HIV-1 tat promoter, as described before [13]. Neutralization studies included 47 heat-inactivated
306 plasmas from infants, 19 bnAbs (PG9, PG16, PGT145, PGDM1400, CAP256.09, CAP256.25, 10-1074,
307 BG18, AIIMS-P01, PGT121, PGT128, PGT135, VRC01, N6, 3BNC117, PGT151, 35O22, 10E8 and 4E10)
308 and 6 non-nAbs (b6, F105, 17b, 48d, A32, 447-52D). Briefly, envelope pseudoviruses were incubated
309 in presence of serially diluted heat inactivated plasmas, bnAbs or non-nAbs for one hour. After
310 incubation, freshly Trypsinized TZM-bl cells were added, with 25 µg/ml DEAE-Dextran. The plates
311 were incubated for 48h at 37°C, cells were lysed in presence of Bright Glow reagent, and
312 luminescence was measured. Using the luminescence of serially diluted bnAbs or plasma, a non-
313 linear regression curve was generated and titres were calculated as the bnAb concentration, or
314 reciprocal dilution of serum that showed 50% reduction in luminescence compared to untreated
315 virus control. For plasma samples, percent neutralization for each plasma-virus combination was
316 recorded as a breadth-potency matrix at a fixed dilution of 1/50: >80% neutralization received a
317 score of 3, >50% a score of 2, >20% a score of 1, and <20 received a score of 0. Maximum cumulative
318 score for a given plasma was 36, and neutralization score was given as the ratio of cumulative score
319 for respective plasma to the maximum cumulative score, providing neutralization score on a
320 continuous matrix of 0 to1, with values closer to 1 implying strong plasma neutralization activity. For
321 epitope mapping, HIV-25710-2.43 pseudoviruses with key mutations within major bnAb epitopes
322 were used [13], and greater than 3-fold reduction in ID50 titres were classifies as dependence. HIV-
323 25710-2.43 mutants included N160K (V2-apex), N332K (V3-glycan), R456W (CD4 binding site),
324 A512W-G514W (Interface) and W672L-F673L (MPER). Extended mapping with N160K mutants of
325 16055_2_3, CAP45_G3 and BG505_W6M_C2, and N332K mutants of CAP256_SU, BG505_W6M_C2,
326 and ConC was performed for samples that showed V2-apex and V3-glycan dependence respectively.

327 **Depletion of MPER plasma antibodies and binding ELISAs**

328 4 wells in 96-well ELISA plates were coated with MPER-C peptide overnight at 4°C. 100 µl of plasma
329 was added and following a 45-minute incubation, plasma was iteratively adsorbed in the remaining
330 three wells. MPER binding ELISA was performed as described previously [13]. Briefly, 96 well ELISA
331 plates (Corning, USA) was coated with 2 µg/ml of MPER-C peptides overnight at 4°C. Coated plates
332 were washed with PBS containing 0.05% Tween 20. Plates were blocked with 5% skimmed milk in
333 blocking buffer. A 50-fold dilution of plasmas, was added, titrated in 2-fold dilution series, and
334 incubated at 37°C for I hour. Unbound plasma antibodies were washed with wash buffer and plates

335 were incubated with peroxidase conjugated goat anti-human IgG at a dilution of 1:1000. Following
336 secondary antibody incubation, the wells were washed, and TMB substrate was added. After color
337 development, reaction was stopped with 0.2 M H_2SO_4 and absorbance was measured at 405 nm.

338 **HIV-1 envelope sequences and phylogenetic analysis**

339 HIV-1 envelope genes were PCR amplified from plasma viral RNA by single genome amplification and
340 directly sequenced commercially. Individual sequence fragments of SGA amplified amplicons were
341 assembled using Sequencher 5.4 (Gene Code Corporation). Subtyping for SGA sequences was
342 performed with REGA HIV subtyping tool (400bp sliding window with 200bp steps size). Inter-clade
343 recombination was examined with RIP 3.0 (Recombinant Identification Program) and with jpHMM.
344 Nucleotide sequences were aligned with MUSCLE in MEGA X. Maximum-likelihood trees were
345 computed with MEGA X using a general-time reversal substitution model incorporating a discrete
346 gamma distribution with 5 invariant sites. Evolutionary divergence within each infant's SGA
347 sequence was conducted in MEGA X and was calculated as number of base substitutions per site
348 from averaging over all sequence pairs. Analyses were conducted using the Maximum Composite
349 Likelihood model. The rate variation among sites was modelled with a gamma distribution (shape
350 parameter = 5). This analysis involved 18 nucleotide sequences. Codon positions included were
351 1st+2nd+3rd+Noncoding. All ambiguous positions were removed for each sequence pair (pairwise
352 deletion option). There were a total of 2622 positions in the final dataset.

353 **Nucleotide sequence accession numbers**

354 The SGA amplified HIV-1 envelope sequences used for inference of phylogeny and highlighter plots
355 are available at GenBank with accession numbers MN703343 – MN703404.

356 **Cloning of autologous HIV-1 envelope genes and production of replication incompetent**
357 **pseudoviruses**

358 Autologous replication incompetent envelope pseudoviruses were generated from AIIMS704,
359 AIIMS706, AIIMS709 and AIIMS743 (elite neutralizers) as described previously[13]. Briefly, viral RNA
360 was isolated from 140 µl of plasma using QIAamp Viral RNA Mini Kit, reverse transcribed, using gene
361 specific primer OFM19 (5` - GCACTCAAGGCAAGCTTTATTGAGGCTTA – 3`) and Superscript III reverse
362 transcriptase, into cDNA which was used in two-round nested PCR for amplification of envelope
363 gene using High Fidelity Phusion DNA Polymerase (New England Biolabs). The envelope amplicons
364 were purified, and ligated into pcDNA3.1D/V5-His-TOPO vector (Invitrogen). Pseudoviruses were
365 prepared by co-transfecting 1.25 µg of HIV-1 envelope containing plasmid with 2.5 µg of an envelope
366 deficient HIV-1 backbone (PSG3Δenv) vector at a molar ratio of 1:2 using PEI-MAX as transfection

367 reagent in HEK293T cells seeded in a 6-well culture plates. Culture supernatants containing
368 pseudoviruses were harvested 48 hours post-transfection, filtered through 0.4µ filter, aliquoted and
369 stored at -80°C until further use. $TCID_{50}$ was determined by infecting TZM-bl cells with serially diluted
370 pseudoviruses in presence of DEAE-Dextran, and lysing the cells 48 hours post-infection. Infectivity
371 titres were determined by measuring luminescence activity in presence of Bright Glow reagent
372 (Promega).

373 **Flow cytometric analysis of antibody binding to cell surface expressed envs**

374 1.25×10^5 HEK293T cells seeded in a 12-well plate were transiently transfected with 1.25 µg of env-
375 coding plasmids (pcDNA3.1 with cloned env/rev cassettes) using PEI-MAX. 48 hours post-
376 transfection, cells were harvested and per experimental requirement, distributed in 1.5 ml
377 microcentrifuge tubes. For sCD4 triggering, 10 µg/ml of 2-domain sCD4 was added and incubated for
378 30 minutes at room temperature. For monoclonal antibody staining, 10 µg/ml of antibody was used
379 and titrated 2-fold in staining buffer. 100 µl of primary antibody (HIV-1 specific monoclonals) were
380 added to HEK293T cells expressing envs, and incubated for 30 minutes at room temperature. After
381 washing, 100 µl of 1:500 diluted PE conjugated goat anti-human Fc was added, and after 30-minute
382 incubation, cells were acquired on BD LSRFortessa X20. Data was analyzed using FlowJo software
383 (version v10.6.1).

384 **Statistical analysis**

385 Mann-Whitney U test and Kruskal-Wallis test were used for comparison of two and three
386 parameters respectively. All statistical analyses were performed on GraphPad Prism 8. A p-value of
387 <0.05 was considered significant.

388 **Acknowledgments**

389 We thank all the study subjects for participating in this study. We are thankful to NIH AIDS Reagent
390 program for providing HIV-1 envelope pseudovirus plasmids, bnAbs, non-nAbs and their expression
391 plasmids, and TZM-bl cells, and Neutralizing Antibody Consortium (NAC), IAVI, USA for providing
392 bnAbs. We are thankful to Dr. Michel Nussenzweig for providing 10-1074 and BG18 bnAb expression
393 plasmids. This work was funded by Department of Biotechnology, India. The Junior Research
394 Fellowship (January 2016 – December 2018) and Senior Research Fellowship (January 2019 –
395 October 2019) to N.M was supported by University Grants Commission (UGC), India.

396 **Author contributions:** N.M designed the study, performed SGA amplification, pseudovirus cloning,
397 and neutralization assays, analyzed data, wrote the initial manuscript, revised and finalized the
398 manuscript. S.S and A.D contributed to SGA amplification, pseudovirus cloning, and neutralization

assays. S.K and H.C expressed PGDM1400, CAP256.25, BG18, 10-1074 and AIIMS-P01 bnAb. R.S, B.K.D, R.L, and S.K.K, provided the samples from HIV-1 infected infants. R.L and S.K.K provided patient care and management. S.K, H.C, and M.A.M edited and revised the manuscript. K.L designed the study, edited, revised and finalized the manuscript.

Competing interests: The authors declare no competing financial interests.

Data and materials availability: The SGA amplified HIV-1 envelope sequences used for inference of phylogeny and highlighter plots are available at GenBank with accession numbers MN703343 – MN703404.

References

1. Sok, D. & Burton, D. R. Recent progress in broadly neutralizing antibodies to HIV. *Nat. Immunol.* **19**, 1179–1188 (2018).
2. Kwong, P. D. & Mascola, J. R. HIV-1 Vaccines Based on Antibody Identification, B Cell Ontogeny, and Epitope Structure. *Immunity* **48**, 855–871 (2018).
3. Doria-Rose, N. A. *et al.* Developmental pathway for potent V1V2-directed HIV-neutralizing antibodies. *Nature* **509**, 55–62 (2014).
4. Bonsignori, M. *et al.* Analysis of a clonal lineage of HIV-1 envelope V2/V3 conformational epitope-specific broadly neutralizing antibodies and their inferred unmutated common ancestors. *J. Virol.* **85**, 9998–10009 (2011).
5. Anthony, C. *et al.* Cooperation between Strain-Specific and Broadly Neutralizing Responses Limited Viral Escape and Prolonged the Exposure of the Broadly Neutralizing Epitope. *J. Virol.* **91**, (2017).
6. Moore, P. L. *et al.* Evolution of an HIV glycan-dependent broadly neutralizing antibody epitope through immune escape. *Nat. Med.* **18**, 1688–1692 (2012).
7. Muenchhoff, M. *et al.* Nonprogressing HIV-infected children share fundamental immunological features of nonpathogenic SIV infection. *Sci Transl Med* **8**, 358ra125 (2016).
8. Ditse, Z. *et al.* HIV-1 Subtype C-Infected Children with Exceptional Neutralization Breadth Exhibit Polyclonal Responses Targeting Known Epitopes. *J. Virol.* **92**, (2018).
9. Goo, L., Chohan, V., Nduati, R. & Overbaugh, J. Early development of broadly neutralizing antibodies in HIV-1-infected infants. *Nat. Med.* **20**, 655–658 (2014).
10. Ghulam-Smith, M. *et al.* Maternal but Not Infant Anti-HIV-1 Neutralizing Antibody Response Associates with Enhanced Transmission and Infant Morbidity. *mBio* **8**, (2017).
11. Makhdoomi, M. A. *et al.* Evolution of cross-neutralizing antibodies and mapping epitope specificity in plasma of chronic HIV-1-infected antiretroviral therapy-naïve children from India. *J. Gen. Virol.* **98**, 1879–1891 (2017).
12. Kumar, S. *et al.* An HIV-1 broadly neutralizing antibody from a clade C infected pediatric elite neutralizer potently neutralizes the contemporaneous and autologous evolving viruses. *J. Virol.* (2018) doi:10.1128/JVI.01495-18.
13. Mishra, N. *et al.* Viral Characteristics Associated with Maintenance of Elite Neutralizing Activity in Chronically HIV-1 Clade C-Infected Monozygotic Pediatric Twins. *J. Virol.* **93**, (2019).
14. Simonich, C. A. *et al.* HIV-1 Neutralizing Antibodies with Limited Hypermutation from an Infant. *Cell* **166**, 77–87 (2016).
15. Overbaugh, J. Mother-infant HIV transmission: do maternal HIV-specific antibodies protect the infant? *PLoS Pathog.* **10**, e1004283 (2014).
16. deCamp, A. *et al.* Global panel of HIV-1 Env reference strains for standardized assessments of vaccine-elicited neutralizing antibodies. *J. Virol.* **88**, 2489–2507 (2014).

17. Kulkarni, S. S. *et al.* Highly complex neutralization determinants on a monophyletic lineage of newly transmitted subtype C HIV-1 Env clones from India. *Virology* **385**, 505–520 (2009).
18. Khan, L. *et al.* Identification of CD4-Binding Site Dependent Plasma Neutralizing Antibodies in an HIV-1 Infected Indian Individual. *PLoS ONE* **10**, e0125575 (2015).
19. Keele, B. F. *et al.* Identification and characterization of transmitted and early founder virus envelopes in primary HIV-1 infection. *Proc. Natl. Acad. Sci. U.S.A.* **105**, 7552–7557 (2008).
20. Novitsky, V., Moyo, S., Wang, R., Gaseitsiwe, S. & Essex, M. Deciphering Multiplicity of HIV-1C Infection: Transmission of Closely Related Multiple Viral Lineages. *PLoS ONE* **11**, e0166746 (2016).
21. Bar, K. J. *et al.* Wide variation in the multiplicity of HIV-1 infection among injection drug users. *J. Virol.* **84**, 6241–6247 (2010).
22. Chaillon, A. *et al.* Characterizing the multiplicity of HIV founder variants during sexual transmission among MSM. *Virus Evol* **2**, vew012 (2016).
23. de Azevedo, S. S. D. *et al.* Highly divergent patterns of genetic diversity and evolution in proviral quasispecies from HIV controllers. *Retrovirology* **14**, 29 (2017).
24. Leitner, T. & Romero-Severson, E. Phylogenetic patterns recover known HIV epidemiological relationships and reveal common transmission of multiple variants. *Nat Microbiol* **3**, 983–988 (2018).
25. Bons, E., Bertels, F. & Regoes, R. R. Estimating the mutational fitness effects distribution during early HIV infection. *Virus Evol* **4**, vey029 (2018).
26. Hraber, P., Korber, B., Wagh, K., Montefiori, D. & Roederer, M. A single, continuous metric to define tiered serum neutralization potency against HIV. *Elife* **7**, (2018).
27. Moore, P. L. *et al.* Potent and broad neutralization of HIV-1 subtype C by plasma antibodies targeting a quaternary epitope including residues in the V2 loop. *J. Virol.* **85**, 3128–3141 (2011).
28. Landais, E. *et al.* Broadly Neutralizing Antibody Responses in a Large Longitudinal Sub-Saharan HIV Primary Infection Cohort. *PLoS Pathog.* **12**, e1005369 (2016).
29. Wibmer, C. K. *et al.* Viral escape from HIV-1 neutralizing antibodies drives increased plasma neutralization breadth through sequential recognition of multiple epitopes and immunotypes. *PLoS Pathog.* **9**, e1003738 (2013).
30. Andrabi, R. *et al.* Identification of Common Features in Prototype Broadly Neutralizing Antibodies to HIV Envelope V2 Apex to Facilitate Vaccine Design. *Immunity* **43**, 959–973 (2015).
31. Kumar, A. *et al.* Infant transmitted/founder HIV-1 viruses from peripartum transmission are neutralization resistant to paired maternal plasma. *PLoS Pathog.* **14**, e1006944 (2018).
32. Kishko, M. *et al.* Genotypic and functional properties of early infant HIV-1 envelopes. *Retrovirology* **8**, 67 (2011).
33. Luan, H. *et al.* Dual Infection Contributes to Rapid Disease Progression in Men Who Have Sex With Men in China. *J. Acquir. Immune Defic. Syndr.* **75**, 480–487 (2017).
34. Bhiman, J. N. *et al.* Viral variants that initiate and drive maturation of V1V2-directed HIV-1 broadly neutralizing antibodies. *Nat. Med.* **21**, 1332–1336 (2015).
35. Gao, Y., Tian, W., Han, X. & Gao, F. Immunological and virological characteristics of human immunodeficiency virus type 1 superinfection: implications in vaccine design. *Front Med* **11**, 480–489 (2017).
36. Kouyos, R. D. *et al.* Tracing HIV-1 strains that imprint broadly neutralizing antibody responses. *Nature* **561**, 406–410 (2018).
37. Sheward, D. J. *et al.* HIV Superinfection Drives De Novo Antibody Responses and Not Neutralization Breadth. *Cell Host Microbe* **24**, 593-599.e3 (2018).
38. Wagner, G. A. *et al.* Intrasubtype B HIV-1 Superinfection Correlates with Delayed Neutralizing Antibody Response. *J. Virol.* **91**, (2017).
39. van Schooten, J. & van Gils, M. J. HIV-1 immunogens and strategies to drive antibody responses towards neutralization breadth. *Retrovirology* **15**, 74 (2018).

494 40. Havenar-Daughton, C., Lee, J. H. & Crotty, S. Tfh cells and HIV bnAbs, an immunodominance
495 model of the HIV neutralizing antibody generation problem. *Immunol. Rev*. **275**, 49–61 (2017).
496

497

Figures and Tables

A

Infant ID	Age (M)	398F1 (A)	TRO11 (B)	X2278 (B)	25710 (C)	CE0217 (C)	CE1176 (C)	X1632 (G)	246F3 (AC)	CNE8 (AE)	CNE55 (AE)	BJOX2000 (BC)	CH119 (BC)	MuLV	Cross-clade nAbs	% Breadth	Geometric Mean Titres	Neutralization Score
AIIMS704	12	245	127	164	324	312	149	228	176	172	186	228	186	<50	+	100	200	0.85
AIIMS706	9	174	<50	158	209	248	144	147	193	122	151	162	316	<50	+	92	177	0.73
AIIMS709	14	152	153	161	244	139	168	152	147	<50	159	148	153	<50	+	92	160	0.72
AIIMS743	14	196	189	153	357	205	105	145	200	<50	99	152	94	<50	+	92	160	0.71
AIIMS731	9	141	117	181	268	<50	<50	113	207	63	<50	127	73	<50	+	75	130	0.52
AIIMS719	12	112	<50	127	321	87	<50	102	212	<50	<50	116	96	<50	+	67	133	0.50
AIIMS736	9	156	<50	154	42	<50	107	118	161	<50	<50	<50	<50	<50	+	50	166	0.49
AIIMS744	14	68	<50	<50	297	94	<50	<50	198	<50	146	163	<50	<50	+	50	144	0.44
AIIMS732	7	124	78	88	112	<50	112	<50	102	<50	<50	<50	<50	<50	+	50	101	0.37
AIIMS738	11	74	85	<50	128	195	147	99	<50	<50	<50	<50	<50	<50	+	50	115	0.36
AIIMS721	24	<50	126	148	181	117	176	<50	<50	<50	<50	<50	<50	<50	+	42	147	0.27
AIIMS703	9	91	62	<50	114	91	<50	<50	<50	<50	<50	<50	<50	<50	+	33	93	0.22
AIIMS705	6	89	<50	<50	158	<50	102	<50	<50	<50	<50	118	<50	<50	+	33	99	0.21
AIIMS707	24	<50	<50	64	126	<50	<50	<50	<50	<50	<50	88	<50	<50	+	25	109	0.18
AIIMS733	12	<50	87	<50	254	<50	<50	<50	110	89	<50	<50	<50	<50	+	33	147	0.17
AIIMS742	19	76	<50	<50	114	<50	<50	<50	<50	<50	<50	<50	<50	<50	+	17	103	0.17
AIIMS716	24	116	<50	99	102	<50	<50	<50	89	<50	<50	<50	<50	<50	+	33	101	0.15
AIIMS720	9	<50	<50	<50	135	112	<50	<50	<50	<50	<50	128	<50	<50	+	25	106	0.13
AIIMS702	24	<50	<50	<50	89	<50	<50	<50	78	<50	<50	81	<50	<50	+	25	92	0.12
AIIMS727	8	<50	<50	<50	112	<50	<50	<50	<50	<50	<50	<50	<50	<50	-	8	113	0.11
AIIMS735	8	<50	<50	<50	118	<50	<50	<50	<50	<50	<50	<50	<50	<50	-	8	102	0.11
AIIMS741	9	<50	<50	<50	186	<50	<50	<50	<50	<50	<50	<50	<50	<50	-	8	152	0.11
AIIMS711	7	<50	<50	<50	174	<50	<50	<50	<50	<50	<50	<50	<50	<50	-	8	106	0.08
AIIMS717	8	<50	<50	<50	115	<50	<50	<50	<50	<50	<50	<50	<50	<50	-	8	99	0.08
AIIMS718	11	<50	<50	<50	116	<50	<50	<50	<50	<50	<50	<50	<50	<50	-	8	91	0.07
AIIMS712	19	<50	<50	<50	89	<50	<50	<50	<50	<50	<50	<50	<50	<50	-	8	112	0.05
AIIMS737	8	<50	<50	<50	76	<50	<50	<50	<50	<50	<50	<50	<50	<50	-	8	119	0.05
AIIMS747	7	<50	<50	<50	78	63	<50	<50	<50	<50	<50	<50	<50	<50	-	17	70	0.03
AIIMS713	12	<50	<50	<50	91	<50	<50	<50	<50	<50	<50	<50	<50	<50	-	8	88	0.03
AIIMS715	8	<50	<50	<50	98	<50	<50	<50	<50	<50	<50	<50	<50	<50	-	8	85	0.03
AIIMS701	24	<50	<50	<50	91	<50	<50	<50	<50	<50	<50	<50	<50	<50	-	8	91	0.02
AIIMS722	13	<50	<50	<50	98	<50	<50	<50	<50	<50	<50	<50	<50	<50	-	8	98	0.02
AIIMS723	12	<50	<50	<50	89	<50	<50	<50	<50	<50	<50	<50	<50	<50	-	8	89	0.02
AIIMS724	14	<50	<50	<50	78	<50	<50	<50	<50	<50	<50	<50	<50	<50	-	8	78	0.02
AIIMS726	18	<50	<50	<50	67	<50	<50	<50	<50	<50	<50	<50	<50	<50	-	8	67	0.02
AIIMS708	18	<50	<50	<50	<50	<50	<50	<50	<50	<50	<50	<50	<50	<50	-	0	0	0
AIIMS714	20	<50	<50	<50	<50	<50	<50	<50	<50	<50	<50	<50	<50	<50	-	0	0	0
AIIMS710	6	<50	<50	<50	<50	<50	<50	<50	<50	<50	<50	<50	<50	<50	-	0	0	0
AIIMS725	9	<50	<50	<50	<50	<50	<50	<50	<50	<50	<50	<50	<50	<50	-	0	0	0
AIIMS728	8	<50	<50	<50	<50	<50	<50	<50	<50	<50	<50	<50	<50	<50	-	0	0	0
AIIMS729	14	<50	<50	<50	<50	<50	<50	<50	<50	<50	<50	<50	<50	<50	-	0	0	0
AIIMS730	18	<50	<50	<50	<50	<50	<50	<50	<50	<50	<50	<50	<50	<50	-	0	0	0
AIIMS748	9	<50	<50	<50	<50	<50	<50	<50	<50	<50	<50	<50	<50	<50	-	0	0	0
AIIMS734	24	<50	<50	<50	<50	<50	<50	<50	<50	<50	<50	<50	<50	<50	-	0	0	0
AIIMS739	17	<50	<50	<50	<50	<50	<50	<50	<50	<50	<50	<50	<50	<50	-	0	0	0
AIIMS740	24	<50	<50	<50	<50	<50	<50	<50	<50	<50	<50	<50	<50	<50	-	0	0	0
AIIMS746	24	<50	<50	<50	<50	<50	<50	<50	<50	<50	<50	<50	<50	<50	-	0	0	0

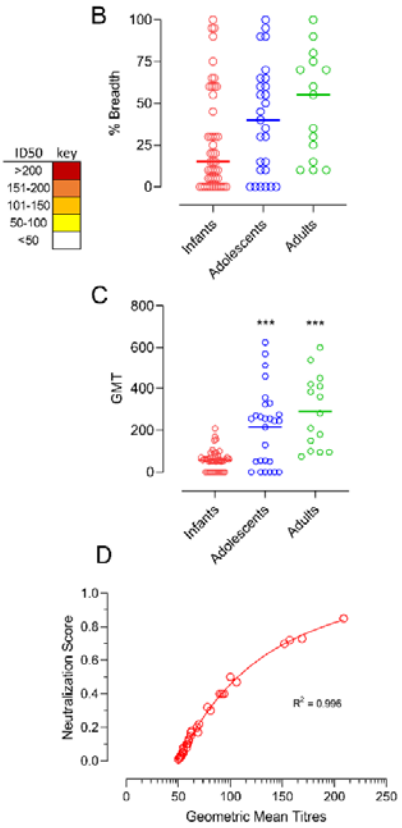

Fig. 1 – Identification of plasma bnAb-inducing infants. (A) Heatmap representing HIV-1 specific neutralization titres (inverse plasma dilution) of plasma nAbs from 47 infant samples against the 12-virus global panel. ID50 values are color-coded per the key given, with darker colors implying higher ID50 titres. (B and C) Comparison of breadth (pseudoviruses showing >50% neutralization at 1/50 plasma dilution) and geometric mean titres of infants with previously established cohorts of chronically infected children (labelled 'adolescents') and adults. (D) Modified neutralization scores predict geometric mean titres.

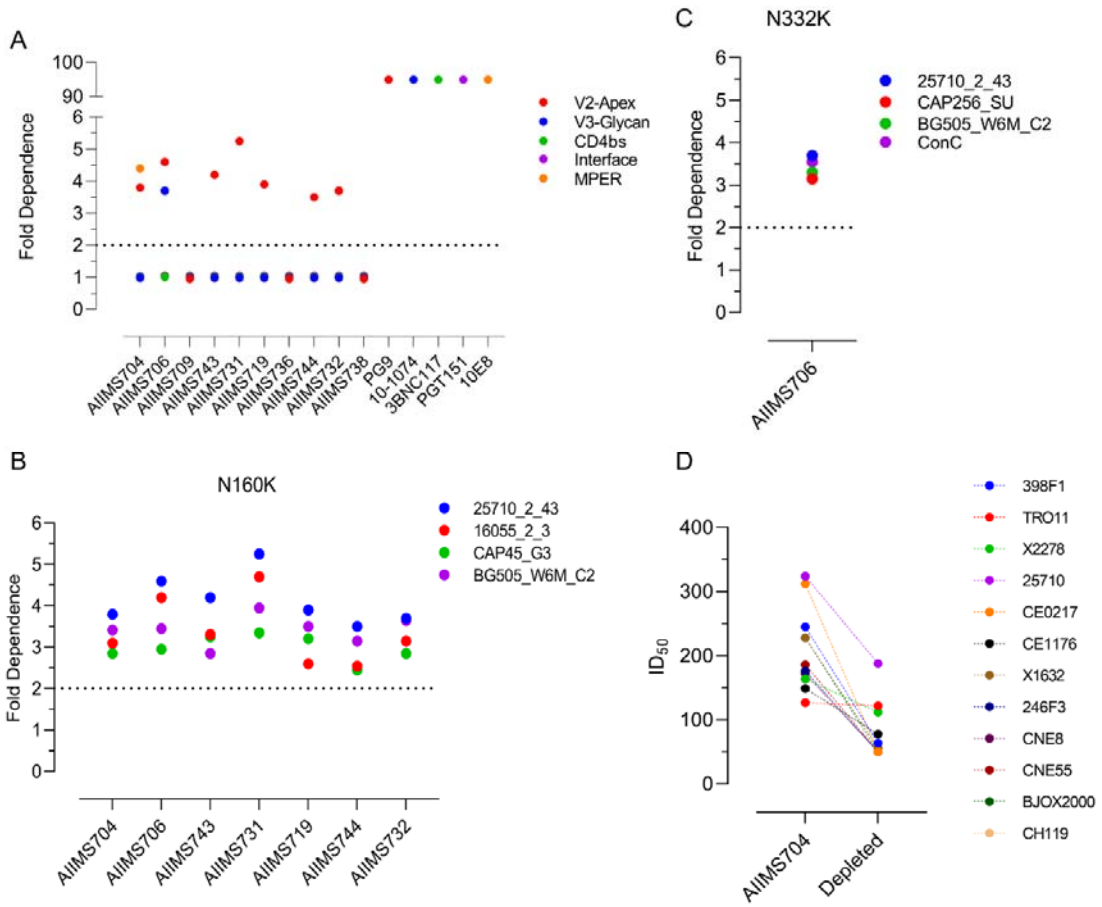

Fig. 2 – V2-apex targeting plasma nAbs predominate in HIV-1 infected infants. (A) Epitope mapping done by mutant viruses in HIV-25710_2_43 backbone for V2-apex (N160K), V3-glycan (N332A), CD4bs (R456W), Interface (A512W-G514W) and MPER (W672L-F673L). PG9 (V2-apex), 10-1074 (V3-glycan), 3BNC117 (CD4bs), PGT151 (Interface) and 10E8 (MPER) bnAbs were used as positive controls. (B) V2-apex (N160K) dependence of infants with diverse pseudoviral backbones. (C) V3-glycan (N332K) dependence of AIIMS706 plasma nAbs against diverse pseudoviral backbone. (D) Comparison of ID_{50} titres of AIIMS704 plasma (undepleted) and MPER-peptide depleted plasma against the 12-virus global panel.

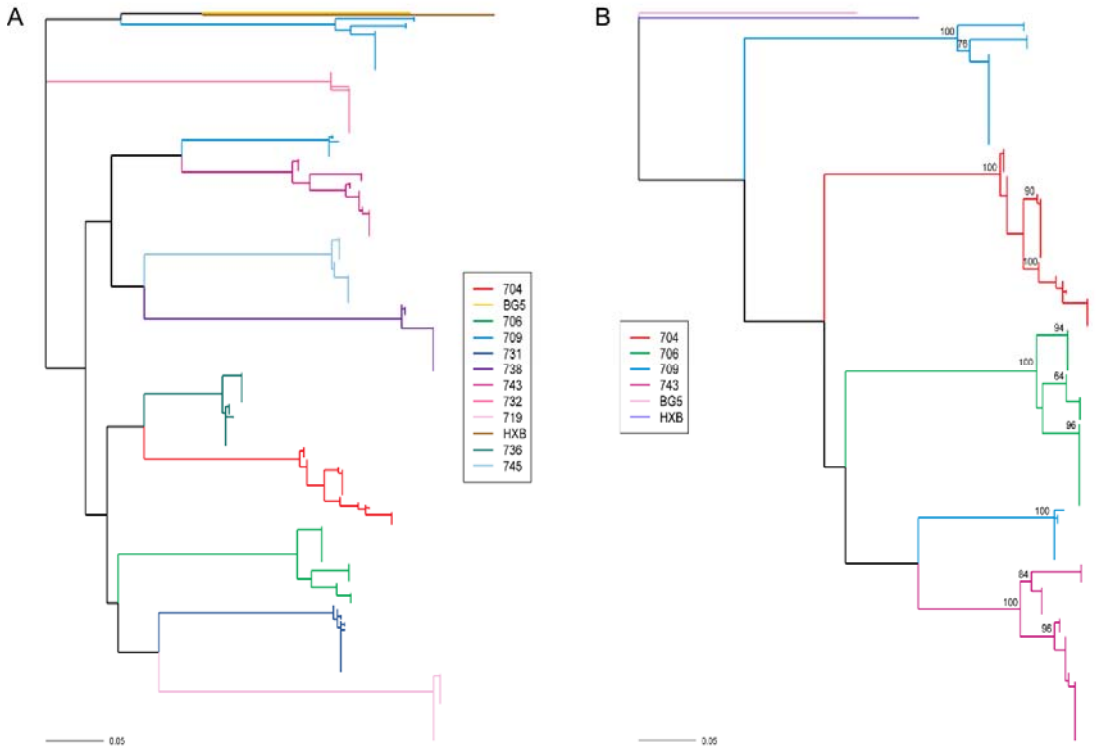

516

517 **Fig. 3 – Multivariant infection in infants with elite plasma neutralizing activity.** (A) Maximum-
518 likelihood tree of env SGA amplicons (V2C5 region, HXB2 position 6690 – 7757) of circulating viral
519 variants from infants with elite and broad plasma neutralizing activity. BG505.W6M.C2 (Clade A,
520 labelled BG5, yellow) and HXB2 (Clade B, labelled HXB, brown) were used as outgroups. Distinct
521 multiple branches for AIIMS704 (red), AIIMS706 (green) AIIMS709 (blue), and AIIMS743 (deep pink)
522 were observed. (B) Maximum-likelihood tree of full length env sequences (HXB2 position 6225 –
523 8795) from the four elite neutralizers (AIIMS704, red; AIIMS706, green; AIIMS709, blue; and
524 AIIMS743, deep pink). BG505.W6M.C2 (Clade A, labelled BG5, light pink) and HXB2 (Clade B, labelled
525 HXB, purple) were used as outgroups. The numerals at the node represent bootstrap value. The
526 horizontal scale bar represents genetic distance. nt, nucleotide.

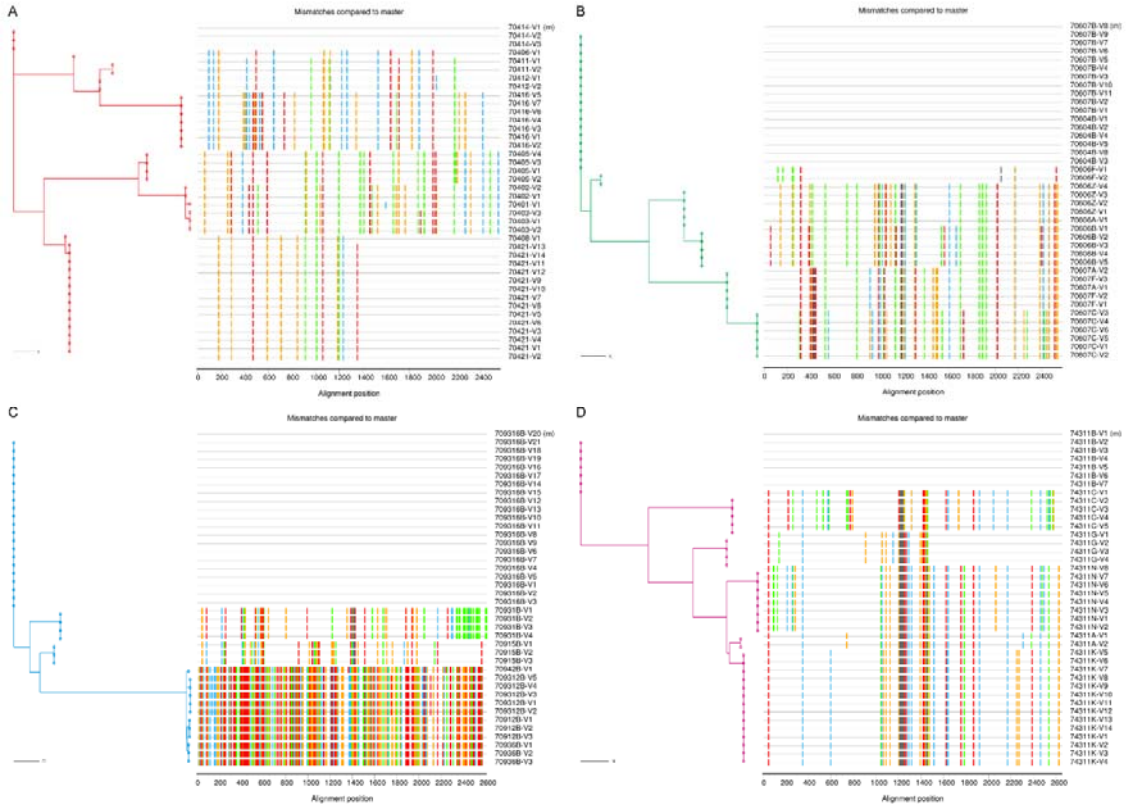

Fig. 4 – Distinct circulating viral variants in infant elite neutralizers. (A – D) Highlighter plots with maximum-likelihood trees of 40 SGA env sequences from each infant suggests productive infection with more than 2 distinct viruses. Maximum-likelihood trees are color coded (AIIMS704 – red, AIIMS706 – Green, AIIMS709 – Blue and AIIMS743 – Deep pink). Colored hash marks on each highlighter plot represent nucleotide difference (A – green; T – red, C – blue, and G – orange) compared to the sequence at the top of the plot. The horizontal scale bar represents genetic distance. nt, nucleotide.

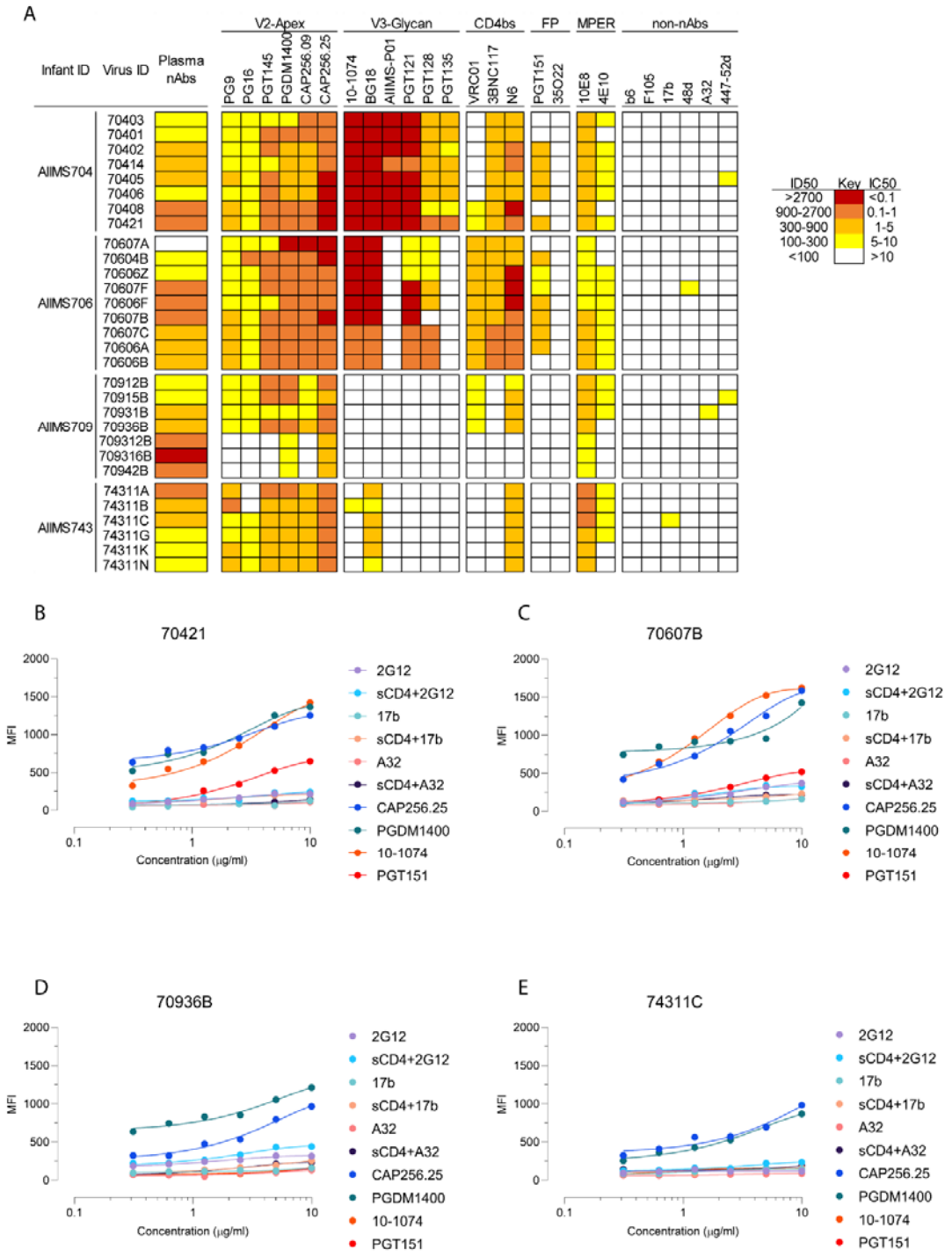

Fig. 5 –Neutralization profile and antigenic characteristics of pseudoviruses from infant elite neutralizers. (A) Neutralization susceptibility of circulating viruses from elite neutralizers to autologous plasma nAbs and known bnAbs was assessed using TZM-bl cells. The potency of plasma and bnAbs is color coded per the key given. Most potent neutralization was seen with V2-apex targeting bnAbs. (B – E) Surface binding assay with varying concentration of trimer specific V2-apex targeting bnAbs (PGDM1400, CAP256.25), V3-glycan targeting bnAb 10-1074, gp120-gp41 interface targeting bnAb PGT151, CD4-induced nnAbs (17b and A32, in presence and absence of sCD4), and

543 gp120 outer domain targeting bnAb (2G12, in presence and absence of sCD4). All binding
544 experiments were repeated thrice, and shown are the average MFI values. MFI, mean fluorescence
545 intensity.

Infant_ID	Neutralization Category	CD4 Count	Plasma Viral Load (Log)	SGA Amplicons (n)	Sex	Circulating Variant	env gene diversity	env divergence
AIIMS704	Elite	2592	5.59	41	M	4	2.5 (0.6-3.2)	0.026
AIIMS706	Elite	1652	5.62	40	M	3	2.4 (0.4-3.6)	0.029
AIIMS709	Elite	2142	5.33	40	M	4	15.1 (0.4-16.6)	0.097
AIIMS743	Elite	1540	5.81	40	M	4	2.6 (0.4-3.5)	0.022
AIIMS731	Broad	1228	5.62	35	M	1	0.6 (0.1-1.5)	0.002
AIIMS719	Broad	1634	5.07	35	F	1	0.3 (0.1-0.7)	0.004
AIIMS736	Broad	2105	6.04	37	F	1	0.6 (0.6-1.2)	0.002
AIIMS744	Broad	2595	5.89	38	M	1	0.6 (0.2-1.1)	0.002
AIIMS732	Broad	1698	6.31	35	M	1	0.7 (0.6-1.3)	0.003
AIIMS738	Broad	1642	4.59	36	M	1	0.6 (0.3-0.77)	0.003

546

547 **Table 1 – HIV-1 env analysis of infant elite and broad neutralizers.** Circulating variants were
548 estimated based on highlighter and bootstrapped neighbour-joining trees (Figure 3A – B and Figure
549 4A – D). env divergence (average evolutionary divergence) among SGA amplicons for each infant was
550 measured as the number of base substitutions per site from averaging over all sequence pairs within
551 each group. env diversity (mean genetic distance) for each infant is shown as median with range,
552 median (range). M – male, F – female.

553

554 **Supplementary Materials**

A

Infant ID	Age (M)	C								% Breadth	Geometric Mean Titres
		25710	25711	1428	16055	330.16.E6	SV21A	ST5B	329.14.B1		
AIIMS704	12	324	321	216	162	221	314	297	201	100	250
AIIMS706	9	209	189	254	138	152	369	164	164	100	195
AIIMS709	14	244	281	331	134	224	101	201	171	100	192
AIIMS743	14	357	227	291	113	247	101	252	204	100	207
AIIMS731	9	268	86	124	61	89	97	249	249	100	135
AIIMS719	12	321	310	258	136	112	164	102	118	100	178
AIIMS736	9	421	160	235	103	214	<50	<50	150	75	193
AIIMS744	14	297	89	103	117	144	118	<50	161	88	136
AIIMS732	7	112	110	259	141	137	132	94	112	100	139
AIIMS738	11	128	<50	<50	84	163	102	149	114	75	120
AIIMS721	24	181	66	114	88	162	164	<50	87	87	116
AIIMS703	9	114	247	88	74	84	78	<50	86	87	100
AIIMS705	6	158	87	118	72	87	81	<50	<50	75	97
AIIMS707	24	126	176	<50	<50	<50	91	146	<50	50	131
AIIMS733	12	254	<50	177	<50	264	<50	<50	<50	38	228
AIIMS742	19	114	<50	247	89	110	<50	<50	58	63	110
AIIMS716	24	102	<50	<50	<50	156	64	<50	<50	38	101
AIIMS720	9	135	<50	<50	<50	77	91	<50	<50	38	98
AIIMS702	24	89	<50	147	<50	88	82	<50	<50	50	99
AIIMS727	8	112	157	88	<50	105	<50	<50	<50	50	113
AIIMS735	8	118	138	68	<50	98	<50	<50	<50	50	102
AIIMS741	9	186	<50	214	<50	88	<50	<50	<50	38	152
AIIMS711	7	174	<50	152	64	<50	74	<50	<50	50	106
AIIMS717	8	115	97	<50	86	<50	<50	<50	<50	38	99
AIIMS718	11	116	<50	73	89	<50	<50	<50	<50	38	91
AIIMS712	19	89	<50	141	<50	<50	<50	<50	<50	25	112
AIIMS737	8	76	<50	186	<50	<50	<50	<50	<50	25	119
AIIMS747	7	78	<50	<50	<50	<50	<50	<50	<50	13	78
AIIMS713	12	91	<50	86	<50	<50	<50	<50	<50	25	88
AIIMS715	8	98	74	<50	<50	<50	<50	<50	<50	25	85
AIIMS701	24	91	<50	<50	<50	<50	<50	<50	<50	13	91
AIIMS722	13	98	<50	<50	<50	<50	<50	<50	<50	13	98
AIIMS723	12	89	<50	<50	<50	<50	<50	<50	<50	13	89
AIIMS724	14	78	<50	<50	<50	<50	<50	<50	<50	13	78
AIIMS726	18	67	<50	<50	<50	<50	<50	<50	<50	13	67
AIIMS708	18	<50	<50	<50	<50	<50	<50	<50	<50	0	0
AIIMS714	20	<50	<50	<50	<50	<50	<50	<50	<50	0	0
AIIMS710	6	<50	<50	<50	<50	<50	<50	<50	<50	0	0
AIIMS725	9	<50	<50	<50	<50	<50	<50	<50	<50	0	0
AIIMS728	8	<50	<50	<50	<50	<50	<50	<50	<50	0	0
AIIMS729	14	<50	<50	<50	<50	<50	<50	<50	<50	0	0
AIIMS730	18	<50	<50	<50	<50	<50	<50	<50	<50	0	0
AIIMS748	9	<50	<50	<50	<50	<50	<50	<50	<50	0	0
AIIMS734	24	<50	<50	<50	<50	<50	<50	<50	<50	0	0
AIIMS739	17	<50	<50	<50	<50	<50	<50	<50	<50	0	0
AIIMS740	24	<50	<50	<50	<50	<50	<50	<50	<50	0	0
AIIMS746	24	<50	<50	<50	<50	<50	<50	<50	<50	0	0

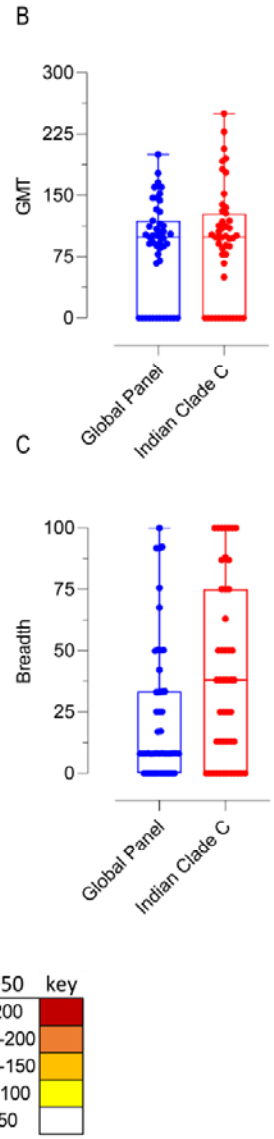

555

556 **Fig. S1 – Plasma Neutralization Activity of HIV-1 infected infants against viral isolates of Indian**
557 **origin.** (A) Heatmap representing HIV-1 specific neutralization titres (inverse plasma dilution) of
558 plasma nAbs from 47 infant samples against the 8-virus Indian clade C panel. ID50 values are color-
559 coded per the key given, with darker colors implying higher ID50 titres. (B and C) Comparison of
560 geometric mean titres and breadth (pseudoviruses showing >50% neutralization at 1/50 plasma

561 dilution) of infants with the 12-virus global panel and 8-virus Indian clade C panel. Data is shown as
562 median with range.

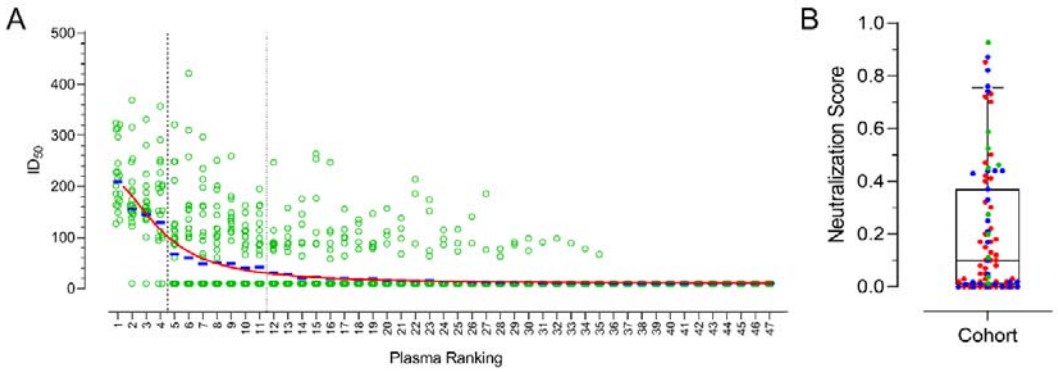

563

564 **Fig. S2 – Neutralization scores calculated based on modified breadth-potency matrix were**
565 **predictive of geometric mean titres.** (A) Infant plasmas are ranked based on geometric mean titres.
566 Green dots represent individual ID50 values against the 12-virus global panel, whereas the blue bar
567 represents geometric mean titres, red line shows non-linear curve fit of modified neutralization
568 score. Neutralization scores accurately predict geometric mean titres. (B) Validation of neutralization
569 score to predict elite and broad neutralizers (red – infants, blue – adolescents and green – adults).
570 Quartile distribution of neutralization scores show 75th percentile at a cut-off of 0.35 and 90th
571 percentile at 0.7. Elite neutralizers typically showed neutralization scores in the 90th percentile,
572 whereas broad neutralizers had a neutralization score in the range of 75th to 90th percentile.

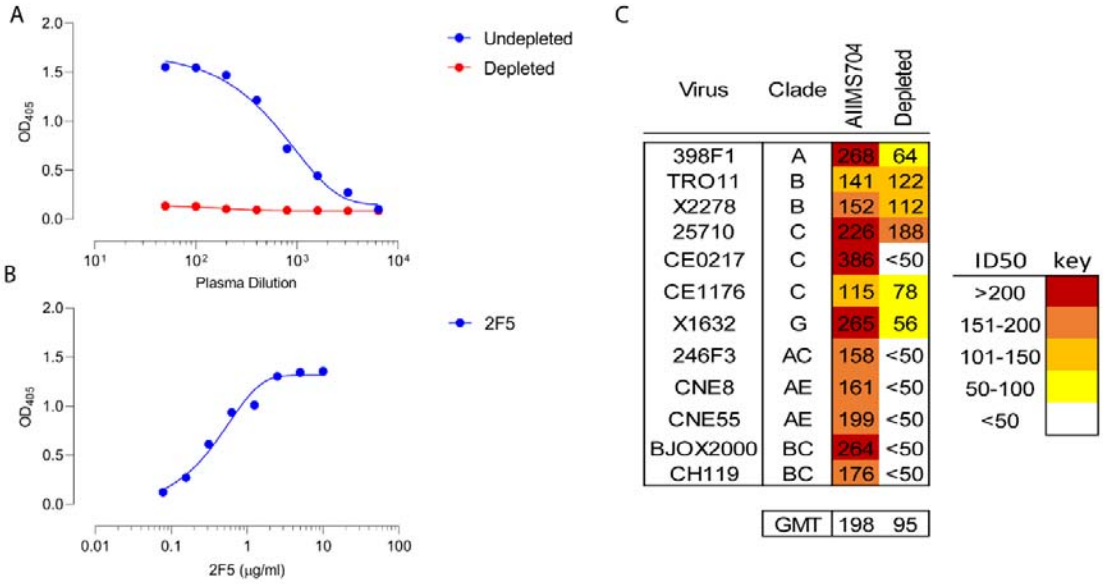

573
574 **Fig. S3 – AIIMS704 had MPER directed plasma bnAbs.** (A) Binding ELISA against MPER-C peptide
575 using undepleted and MPER-C depleted AIIMS704 plasma showed efficient adsorption and depletion
576 of anti-MPER plasma bnAbs. (B) 2F5, an anti-MPER bnAb was used as positive control. (C) ID50
577 values of AIIMS704 undepleted and MPER-C depleted plasma against the 12-virus global panel.
578 MPER depletion resulted in 2-fold reduction in GMT titres.

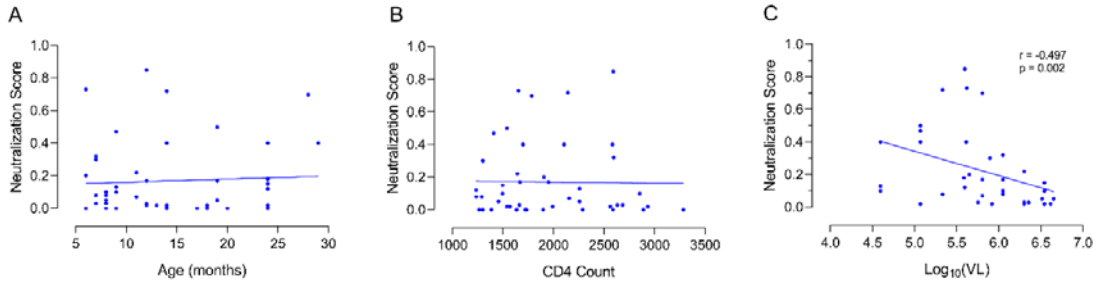

Fig. S4 – Influence of host and viral parameter on neutralization breadth. Correlation between (A) duration of infection, (B) CD4 T-cell counts and (C) viral load with neutralization scores for infants with discernible neutralization activity. Infants that showed no neutralization against the 12-virus global panel were excluded from analysis.

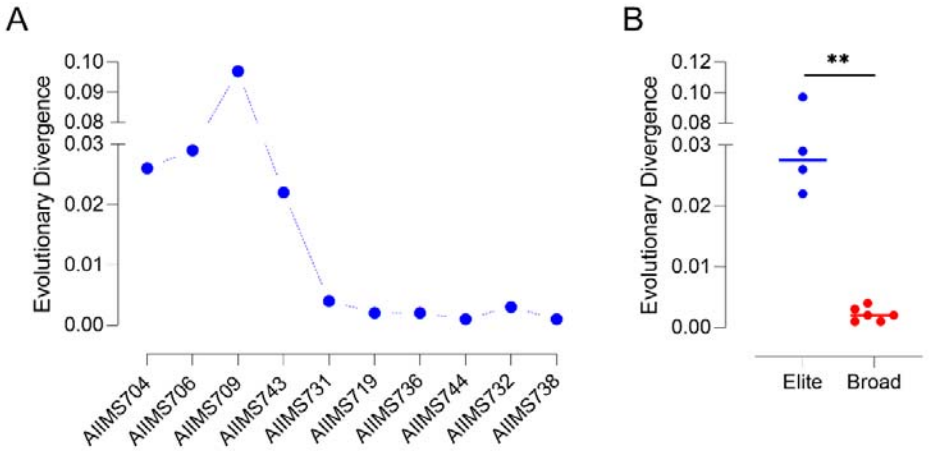

Fig. S5 – Viral population in infant elite neutralizers is highly divergent. (A) Average evolutionary divergence (nucleotide substitutions per site) among SGA amplicons for infant elite and broad neutralizers. The number of base substitutions per site from averaging over all sequence pairs within each group are shown. Analyses were conducted using the Maximum Composite Likelihood model [1]. The rate variation among sites was modelled with a gamma distribution (shape parameter = 5). (B) Statistical comparison between elite and broad neutralizers was conducted by Mann Whitney U test. ** represent a p-value of 0.0095.

Fig. S6 – Frequency plot of the V2-loop sequences of infant elite neutralizers. Weblogo plot showing the amino acid frequency plots of V2-loop (HXB2 amino acids 156 – 177) from SGA amplicons of elite neutralizers. Key glycan (N156 and N160) were well-conserved.

Neutralization	Score	Infants

Category		N (%)
Elite	0.7-1	4 (8.51)
Broad	0.3-0.7	6 (12.27)
Cross	0.1-0.3	9 (19.15)
Weak or none	<0.1	28 (59.57)

596

597 **Table S1 – Categorization of infants with varied viral neutralization activity.** Neutralization
598 categories were defined based on normalized neutralization score against the 12-virus global panel.
599 Scores of ≥0.7 were predictive of elite neutralization activity, scores in the range of 0.3 to 0.7 were
600 predictive of broad neutralization activity, and scores in the range of 0.1 to 0.3 were predictive of
601 cross neutralization activity. N = number of infants.

Infant ID	Clone ID	SGA Clones (Number)
AIIMS704	70401	1
	70402	2
	70403	3
	70405	4
	70406	1
	70408	1
	70411	2
	70412	2
	70414	3
	70416	7
	70421	14
AIIMS706	70607A	2
	70604B	6
	70606Z	4
	70607F	3
	70606F	2
	70607B	11
	70607C	6
	70606A	1
	70606B	5
AIIMS709	70912B	3
	70915B	3
	70931B	4
	70936B	3
	709312B	5
	709316B	21
	70942B	1
AIIMS719	71901A	2
	71904B	9
	71904D	16

	71905G	1
	71906F	7
AIMS731	73105B	4
	73105C	3
	73105H	14
	73106B	2
	73106F	13
	73106G	3
AIIMS732	73201A	3
	73201B	1
	73201C	24
	73201D	4
AIIMS736	73601A	11
	73604D	16
	73602H	2
	73603B	3
	73603D	6
AIIMS738	73801A	1
	73801B	5
	73801C	24
	73801D	5
AIIMS743	74311A	2
	74311B	7
	74311C	5
	74311G	4
	74311K	14
	74311N	8
AIIMS744	74401A	8
	74401C	5
	74401F	4
	74402D	11
	74402E	2

Table S2 – Population frequency of SGA env amplicons from infant elite and broad neutralizers.